Technical Review of PWM Techniques for Dual Active Bridge for EV Charging

P.B. Musiiwa [1,5], E.T. Kapuya [2], D. Musademba [3], D. Simango [4]
[1,3,4] Mechatronics Department, School of Engineering and Technology, Chinhoyi University of Technology
[2]Electrical and Electronic Engineering Department, University of Zimbabwe
[5]Electronic Engineering Department, School of Engineering and Technology, Harare Institute of Technology
[1]pbmusiiwa@gmail.com, [2]engelbert.kapuya@gmail.com , [3]dmusademba@gmail.com , [4]doubtsimango255@gmail.com

Article History

Received: Jan. 12, 2026

Revised: Apr. 12, 2026

Accepted: Jun. 03, 2026

Abstract

The need for bidirectional power flow between Electric Vehicle (EV) chargers and the grid via Vehicle-to-Grid (V2G) technology demands efficient power electronic converters. In modern technology Dual Active Bridge (DAB) has played a pivotal role in the electronic interface (DC–DC) conversion due to its galvanic isolation (High Frequency Transformer (HFT)) structure, bidirectional flow capability, power density, and wide voltage regulation capability. At the core of the efficient operation of the DAB are the Pulse Width Modulation (PWM) techniques. The PWM strategies also extend the zero-voltage switching (ZVS) range and reduce circulating inductive current. This paper reviews and compares the technical aspects of PWM techniques applied in DAB-based EV charging systems, *inter alia*, Phase Shift Modulation (PSM), Combined PWM (CPWM), Dual Phase Shift (DPS), Triangular and Trapezium Modulation (TTM), PWM plus Phase Shift (PWM–PS), and Asymmetric Duty Cycle Control (ADC). The mathematical analysis of the strategies was done using the power transfer equations and loss mechanisms. Performance evaluation was done based on soft-switching range, circulating inductive current, efficiency, and aptness to Electric Vehicle charging needs. The paper concludes that Dual Phase Shift and PWM plus Phase Shift have superior wide voltage variations, which is standard for fast DC charging, but Phase Shift Modulation is simplified for medium-power onboard chargers.

Keywords- Bidirectional DC–DC Converter, Dual Active Bridge, Electric Vehicle Charging, PWM Techniques, Soft Switching.

I. INTRODUCTION

The need for sustainable transportation has changed power electronic interface performance standards, creating the necessity for efficient, high-power-density, and reliable DC-DC conversion phases [1-2]. The Electric Vehicle (EV) charging environments should handle wide battery voltage whilst maintaining galvanic isolation and bidirectional Vehicle-to-Grid (V2G) power flow services [3]. The Dual Active Bridge (DAB) has been a favourite topology in EV charging because of its symmetrical nature, soft-switching capacity, and its modularity. The Pulse Width Modulation (PWM) technique influences the DAB efficiency. Single-Phase Shift (SPS) modulation offers simple DAB control, but is affected by performance degradation, high circulating inductive currents, and a constrained Zero-Voltage Switching (ZVS) range under the voltage mismatch conditions normally found in lithium-ion battery cycles [3,5], which are normally used in EV structures due to the high power-to-weight ratio of lithium-ion chemistries.

Dual Active Bridge Converter Principle

A single-phase DAB converter consists of a primary switching full-bridge, a high-frequency transformer (HFT), a leakage inductance (L_{LK}), and a secondary switching full-bridge shown in Figure 1. The power transfer is controlled by the phase shift between the primary (Bridge 1) and secondary bridge (Bridge 2) voltages [1-5]. The DAB converter leverages high-frequency magnetic coupling to manage bidirectional power flow between two DC sources. The PWM Bridge 1 converts the incoming DC voltage into a high-frequency square wave or quasi-square wave voltage. $(v_P(t))$. This AC $v_p(t)$ signal then passes through the L_{LK}, which serves as the primary energy storage and transfer medium for the entire system. The DAB operation is centered on the Phase Shift (ϕ) between the switching patterns of the primary and secondary bridges. Concurrently, the PWM Bridge 2 generates. $v_s(t)$, which is mirrored to the primary side as $nv_s(t)$. Distinct from the conventional converters that modulate the duty cycle, a Dual Active Bridge characteristically operates with a fixed 50% duty cycle for all the MOSFET switches [7]. Alternatively, the controller establishes a time delay via the phase shift between the two bridges. When the primary bridge leads to the secondary bridge, the phase shift creates a voltage across the leakage inductor that transfers power from the input to the output. Reversing the phase so that the primary bridge lags leads to reversing the current direction and enabling power flow back to the source [8]. The high-frequency transformer (HFT) offers notable

galvanic isolation but scales the voltage corresponding to its turns ratio (1: N). This isolation is vital for safety and noise decoupling in sensitive purposes [8-9]. This topology inherently achieves Zero Voltage Switching (ZVS). During the dead-time intervals between switch transitions, the energy stored in the leakage inductor (L_{LK}), naturally discharges the output capacitance of the MOSFETs. This allows switch activation at zero voltage, drastically reducing switching losses and enabling high-frequency operation and subsequently reduces magnetic components' physical size. Efficiency in a DAB converter is optimized most when the input voltage (V_{IN}) is closely matched to the referred output voltage $\left({}^{V_{OUT}}/_{N}\right)$. When these voltages are balanced, the circulating reactive power is minimized, leading to lower conduction losses in the semiconductor devices and the transformer windings [9-10]. Because the power transfer is inversely proportional to the switching frequency and the leakage inductance, precise tuning of the inductor value is required to balance the maximum power throughput against the desired ZVS operating range [11].

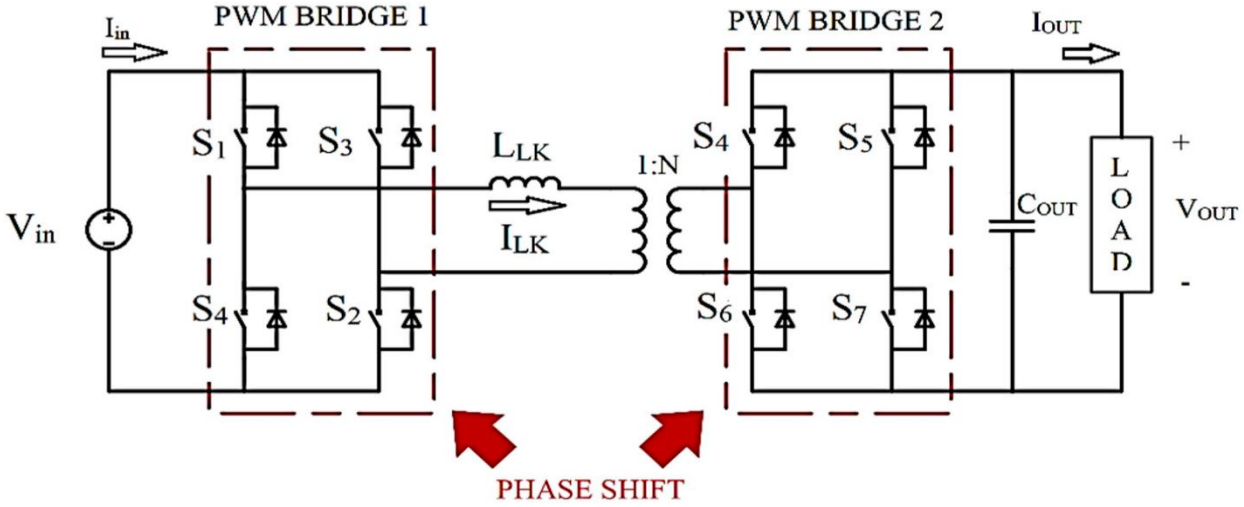

Figure 1: Single phase DAB Converter configuration

Power flow is induced by the instantaneous voltage differential across the series inductor, which governs the high-frequency AC current, $i_L(t)$, according to (1):

$$L\frac{di_L(t)}{dt} = v_p(t) - nv_s(t) \qquad (1)$$

For ideal switches, a unity transformer turns ratio (n = 1), and negligible losses, the average transferred power is given by (2).

$$P = \frac{V_1 V_2}{\omega L}\phi\left(1 - \frac{|\phi|}{\pi}\right) \qquad (2)$$

To be specific, for a lossless DAB converter operating under Single Phase Shift (SPS) modulation, the average power P transferred between the bridges is described by (3)

$$P = \frac{nV_1V_2\phi(\pi - |\phi|)}{2\pi^2 f_s L} \qquad (3)$$

The peak inductor current under PSM is expressed by (4).

$$I_{pk} = \frac{(V_1 - V_2)\phi}{\omega L} \qquad (4)$$

Large inductor current at low power is the main source of circulating losses in conventional PSM [12].

II. PULSE WIDTH MODULATION (PWM) TECHNIQUES

Pulse Width Modulation (PWM) refers to the switching control method in which the duty ratio or relative timing of gate signals is varied to regulate power flow. In DAB converters, PWM not only controls the average power transfer but also determines soft-switching conditions, Root-Mean-Square (RMS) current, and loss distribution [1,8]. PWM functions in DAB control include intensification of ZVS region, minimization of the circulating current, reduction of conduction and switching losses, and improved light-load efficiency [9]. Despite its advantages, the conventional PSM-controlled DAB suffers from high reactive circulating current under light load, limited ZVS under voltage mismatch, reduced efficiency at partial load, and increased semiconductor stress. These limitations stimulate the utilization of advanced PWM techniques tailored to the strict demands of EV charging systems, for instance, a wide battery voltage range, high efficiency (>95%), and V2G power flow [6, 13].

a. Phase Shift Modulation (PSM)

Phase Shift Modulation (PSM), also known as Single-Phase Shift (SPS) control, is the main DAB Converter operational framework with high technical scrutiny due to its non-ideal voltage matching performance degradation. Involves applying a high-frequency two-

square wave to both the primary and secondary bridges of the high-frequency transformer and linkage inductor. The power flow is controlled by the phase displacement angle (ϕ) between these two square waves. The Phase Shift is the relative time delay between the primary voltage (V_1 or V_p) and the secondary voltage ($V_2 or$ V_s) [14]. The instantaneous $i_L(t)$ is driven by the inductor voltage (1), which leads to the power transfer P (5) after integration over a switching period of T_{sw}:

$$P = \frac{V_1 V_2}{2 f_{sw} L d} \phi \left(1 - \frac{|\phi|}{\pi}\right) \quad (5)$$

PSM causes a surge of circulating power and the collapse of the Zero Voltage Switching (ZVS) range when the voltage conversion ratio (6)

$$M = \frac{nV_2}{V_1} \neq 1 \quad (6)$$

If the voltage conversion ratio is unity, the current waveform is purely trapezoidal, and the reactive power component is minimized [15]. However, as it deviates from unity, the phase difference between the voltage and current increases, leading to significant backflow power where energy returns to the source within each half-cycle. This increases the RMS current ($I_{L,rms}$), which scales the conduction losses across the MOSFET $R_{DS(on)}$ and the transformer's AC winding resistance R_{ac} by a factor of I_{rms}^2 [15-16]. Furthermore, the ZVS boundaries are strictly defined by the magnitude of the inductor current at the switching instants; if the current. $i_L(t)$ The turn-off is insufficient to fully discharge the output capacitance C_{oss} of the incoming switch, the converter transitions into hard switching [17]. This results in capacitive turn-on losses defined by (7), creating thermal bottlenecks and necessitating oversized Electromagnetic Interference (EMI) filtering due to high dv/dt transients. In the magnetics view, elevated harmonic content inherent in the PSM square-wave excitation prompts significant proximity and skin effect losses within the HFT [18]. The PSM cannot improve these losses since it uses a single degree of freedom (ϕ).

$$P_{sw} = \frac{1}{2} C_{oss} V^2 f_{sw} \quad (7)$$

b. The Combined Pulse Width Modulation (CPWM) technique

The CPWM technique has a huge architectural shift from Phase Shift Modulation (PSM) as it provides a secondary control variable to the DAB. CPWM varies both the duty cycle and phase shift, presenting a multi-dimensional control space that solves the inherent constraints of SPS modulation [2,19]. In CPWM, the primary and secondary bridges are no longer fixed at 50% as in PSM, implying that the square-wave excitation is flexible [1, 20]. The CPWM produces three-level quasi-square waves instead of two level produced by PSM. This permits the controller to alter the zero-voltage times of the transformer's excitation, thereby decoupling the voltage magnitude from the switching period [21]. These duty cycle parameters effectively alter the power flow equations and make it defined by the interaction of the primary and secondary duty cycles (D_p and D_s) and the phase shift angle ϕ (8).

$$P = \frac{V_1 V_2}{\omega L} (D_P D_S) f(\phi) \quad (8)$$

$f(\phi)$ is the phase shift piecewise function, (9) for normalized regions.

$$f(\phi) = \phi \left(1 - \frac{|\phi|}{\pi}\right) \quad (9)$$

Different from PSM, where D_P and D_S are typically 1, CPWM regulates power (P) via three independent variables, fulfilling the load demand while concurrently optimizing specific performance metrics, such as minimum current stress. The CPWM strategy curtails the circulating current more than PSM [22]. In PSM, when the input (V_1) and output (V_2) voltages do not match the transformer turns ratio, inductor current i_L continues to flow even when it opposes the bridge voltage, resulting in backflow or reactive power. Correct setting of D_P and D_S to zero out the bridge voltage during periods of potential backflow, CPWM minimises the heat $I_{L,rms}^2 R$ loss through curtailing RMS Current [22-24]. The settings also subject the magnetic components to lower peak flux densities. Also, the duty cycles can be tuned to maintain zero-voltage switching across a wider range of operating conditions, particularly at light loads where PSM typically fails (Enhanced ZVS). Although the CPWM offers better efficiency, it imposes a greater computational burden on the controller [23]. Figure 2 outlines the thorough architecture, modulation transitions, and performance improvements of the Combined Pulse Width Modulation (CPWM) technique employed in a DAB converter. As shown in the operational and controller block diagrams (a and b), the CPWM framework dynamically processes the voltage gain command (M), power command (P), and input fundamental phase command (ϕ_f) within a modular transition logic block to switch adaptively between Symmetrical/Single PWM (SPWM) and Dual PWM (DPWM) operational modes, creating a unified control parameter set comprising the primary duty ratio (d_p), modified outer phase shift (ϕ) and secondary duty ratio (d_s). The waveform matrix in (b) shows that by altering these multi-level voltage profiles (V_{ab} and V_{cd_ref}) for the low-gain ($M < 1$) and high-gain ($M > 1$) boundaries, CPWM quashes the severe volt-second imbalances across the high-frequency isolation inductor L that normally plague conventional Phase Shift Modulation (PSM) with fixed 50% duty cycles. Subsequently, the resulting piece-wise inductor current (i_L) is strongly constrained, as validated by the 3D performance optimization surfaces in (c), this hybrid modulation method dramatically limits reactive circulating power, minimizes RMS inductor conduction losses, and obtains a vastly expanded soft-switching ZVS boundary across a wide operating and voltage-variance packet.

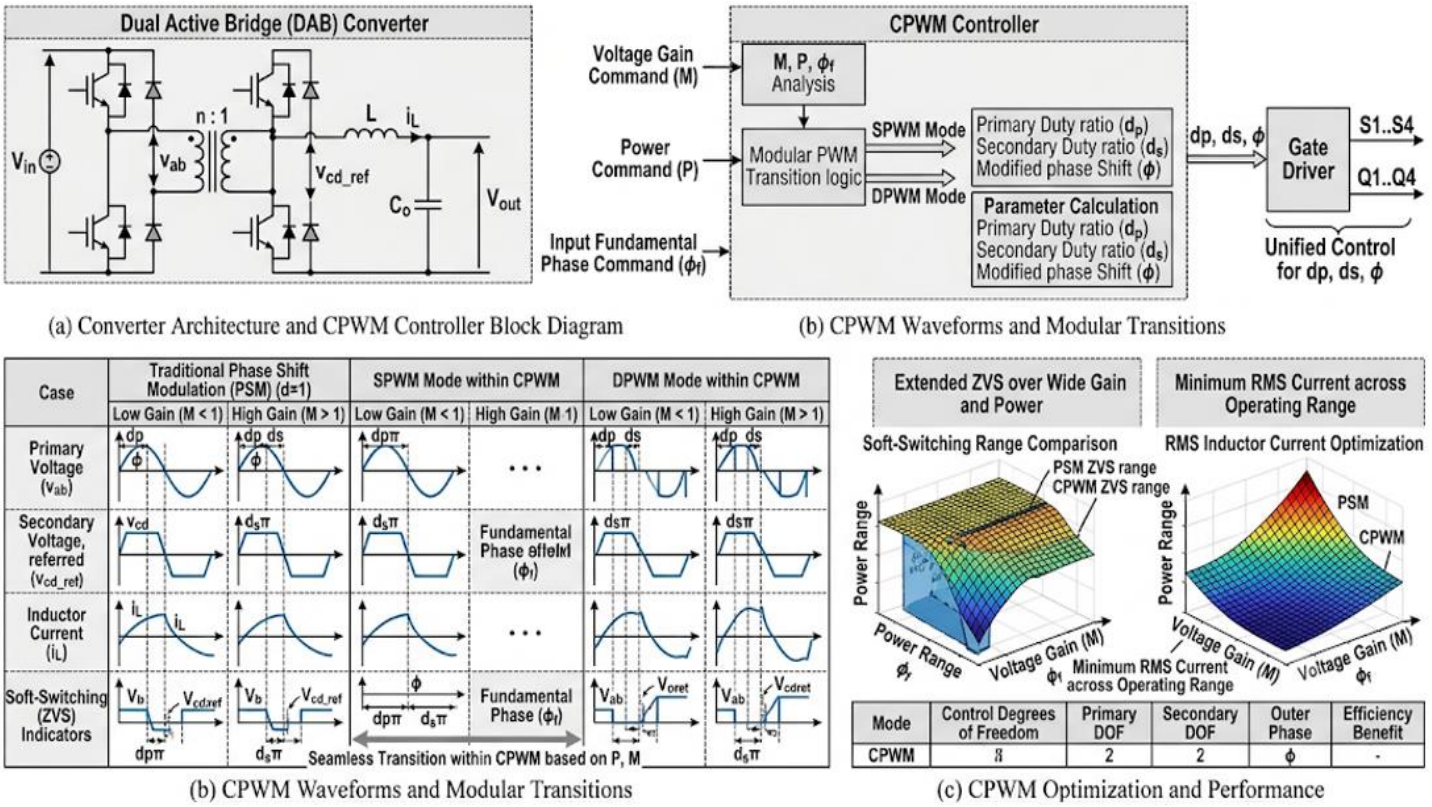

Figure 1: Diagrams showing the Combined Pulse Width Modulation (CPWM) technique in Dual Active Bridge (Ab Malek et al, 2018 and Ab Malek et al, 2019)

c. Dual Phase Shift (DPS) technique

The DPS is a sophisticated modulation strategy that builds upon the limitations of Single-Phase Shift (SPS) by introducing a second control variable to optimize converter performance. Like CPWM in the DPS framework, the primary and secondary bridges are no longer restricted to 50% duty cycle square waves [25]. Unlike universal Phase Shift Modulation (PSM), where only the displacement between bridges is controlled, DPS introduces an inner phase shift that is identical for both the primary and secondary bridges. In the DPS, both bridges share a common internal duty cycle (D_1), while a global phase shift (ϕ) regulates the power flow between the two bridges. This creates a three-level (quasi-square) voltage waveform ($V_1, 0, -V_1$) at the transformer terminals. The power transfer in DPS is mathematically more granular than SPS. Depending on the relationship between the inner Duty-cycle (D_1), and the outer phase shift (ϕ), the power P is expressed through distinct operating modes [26]. For the most common region ($0 \leq D_1 \leq \phi \leq 1$), the power is defined as (10).

$$P = \frac{V_1 V_2}{2\pi f_{sw} L}[\phi(1-\phi) - D_1(1-D_1)] \qquad (10)$$

This indicates that power is no longer solely a function of ϕ, but rather the difference in the squares of the phase shifts, allowing for a more nuanced control of the energy transfer. The DPS technique drastically suppresses the circulating current compared to traditional PSM. In SPS, power is often sent back to the source when $M \neq 1$, leading to high RMS currents that do not contribute to the load. DPS can blank out the portions of the voltage waveforms where backflow would typically occur through the adjustment of D_1. This aligns the inductor current i_L more closely with the voltage phase, minimizing the reactive power component [26]. The reduction of the circulating current curtails $I_{L,rms}^2 R$ conduction losses. DPS significantly outperforms SPS in maintaining Zero Voltage Switching (ZVS). Under light loads, SPS often loses ZVS since the inductor current at the switching instant is insufficient to discharge the switch's output capacitance C_{oss}. The DPS also introduces an additional degree of freedom to maintain the current. i_L is high enough at all switching transitions to enable ZVS, permitting the converter to function effectively across a wider range of voltage ratios (M), which is critical for battery-linked uses where voltages swing substantially [27]. DPS has a computational complexity, which complicates real-time implementation. To attain the highest efficiency, the controller should resolve for the optimal combination of D_1 *and* ϕ for all power levels, presenting the need for expensive fast Digital Signal Processors (DSPs) to handle pre-calculated look-up tables or iterative optimization algorithms. As both the primary and secondary bridges are modulated with an internal phase shift, any minimal asymmetry in the gate driver signals results in HFT DC bias. To avoid core saturation, the DPS requires active flux balancing or high-precision timing [28-29]. Higher harmonic content of the three-level waveform leads to elevated magnetic core eddy current losses compared to a pure square wave [30].

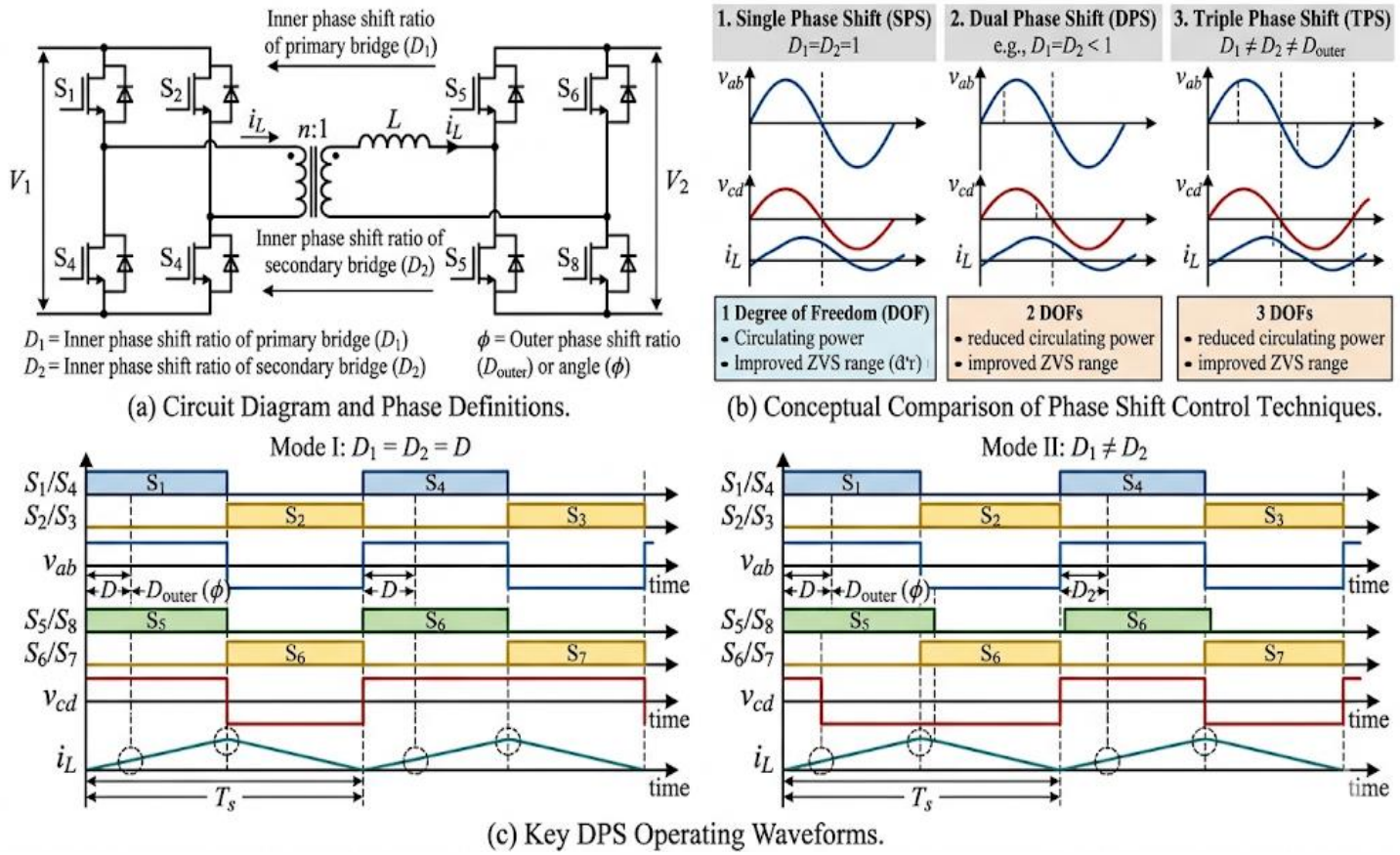

Figure 2: Diagrams for operation of Dual Active Bridge under Dual Phase Shift (DPS) technique (Zhao, B. et al, 2013 and Liu, X. et al 2016)

Figure 3 shows the DAB converter Dual Phase Shift (DPS) modulation, attained by applying identical inner phase shift and a global outer phase shift across the two bridges. Distinct from Extended Phase Shift (EPS) which limits pulse-width modulation to a single bridge, DPS applies a uniform inner phase-shift ratio (d_1) to the primary and secondary full-bridges, thereby shaping the primary AC voltage mutually (v_1) and secondary AC voltage (v_2) into symmetrical three-level waveforms covering equal zero-voltage periods. The second degree of freedom, the outer phase shift (ϕ), defines the relative time displacement between these two three-level waveforms to control the size and direction of the bidirectional power flow. By locking the internal pulse widths of both bridges together, DPS effectively curtails the multi-variable control complexity compared to Triple Phase Shift (TPS) with dynamism minimizing the volt-second mismatch across the high-frequency isolation inductor L. Consequently, the resulting piece-wise linear inductor current (i_LThe trajectory is optimized to eliminate reactive back-flow power and reduce peak and RMS conduction losses during non-unity voltage gain conditions ($V_{in} \neq nV_{out}$), vastly expanding the soft-switching ZVS operational boundaries of the converter.

d. Triangular and Trapezium Modulation (TTM)

Triangular and Trapezium Modulation (TTM) is a DAB converter decisive subset of PSM techniques, overtly designed to eliminate switching losses and reduce reactive power throughout high voltage conversion ratios. Contrasting the SPS which produces a constant trapezoidal current, TTM limits the current waveform to definite shapes to ensure optimal soft switching [6, 31]. TTM is largely used when the voltage conversion ratio M (6) departs extensively from 1. The technique modulates the duty cycles of the primary and secondary bridges (D_P and D_S) and the phase shift (ϕ) such that the inductor current $i_L(t)$ reaches zero at specific switching instants. In Triangular Modulation (TRM), the current i_L starts at zero, rises to a peak, and returns to zero within a half-cycle [7]. This occurs when the phase shift and duty cycles are adjusted so that the inductor does not hold residual energy at the end of the power transfer interval. If $M < 1$ the power P is given by:

$$P = \frac{V_1^2 D_P^2}{2 f_{sw} L} \cdot \frac{M}{1+M} \qquad (11)$$

TRM is normally restricted to low power levels since the peak current required to transfer high power in a "triangular" shape is prohibitively high. Trapezium Modulation **(**TZM) is an extension used for medium power levels. It introduces a zero-current plateau where the current remains at zero for a portion of the switching period. This is achieved by simultaneously varying the duty cycle and phase shift [10]. TTM offers Zero-Current Switching (ZCS) for one or more switching transitions which hypothetically eliminates turn-off losses. This addresses the critique of standard PSM, where the primary and secondary bridge voltages are no longer fixed at

50% duty, allowing for a broader soft-switching envelope. TTM is possibly the most efficient technique to handle Backflow Power. By ensuring the current never flows against the voltage polarity, the circulating current is significantly reduced compared to PSM. This leads to a drastic reduction in RMS current. $I_{L,rms}$, which optimizes the conduction losses in the MOSFET $R_{DS(on)}$ and transformer windings. The mathematical trade-off in TTM is the requirement for a higher peak current (I_{pk}). To transfer the same average power P as a square-wave (SPS), a triangular or trapezoidal wave requires a significantly higher peak [32-34]. This increases the saturation requirements for the high-frequency transformer core. It places higher instantaneous stress on the semiconductor devices, potentially requiring higher-rated (and more expensive) MOSFETs. Implementing TTM requires the controller to switch between different modulation modes (SPS, DPS, and TTM) depending on the load. Moving from TTM (light load) to SPS (heavy load) creates control discontinuities that can lead to transient oscillations in the output voltage [35]. The power P transfer expression under CPWM/TTM (8), requires real-time calculation of three independent variables.

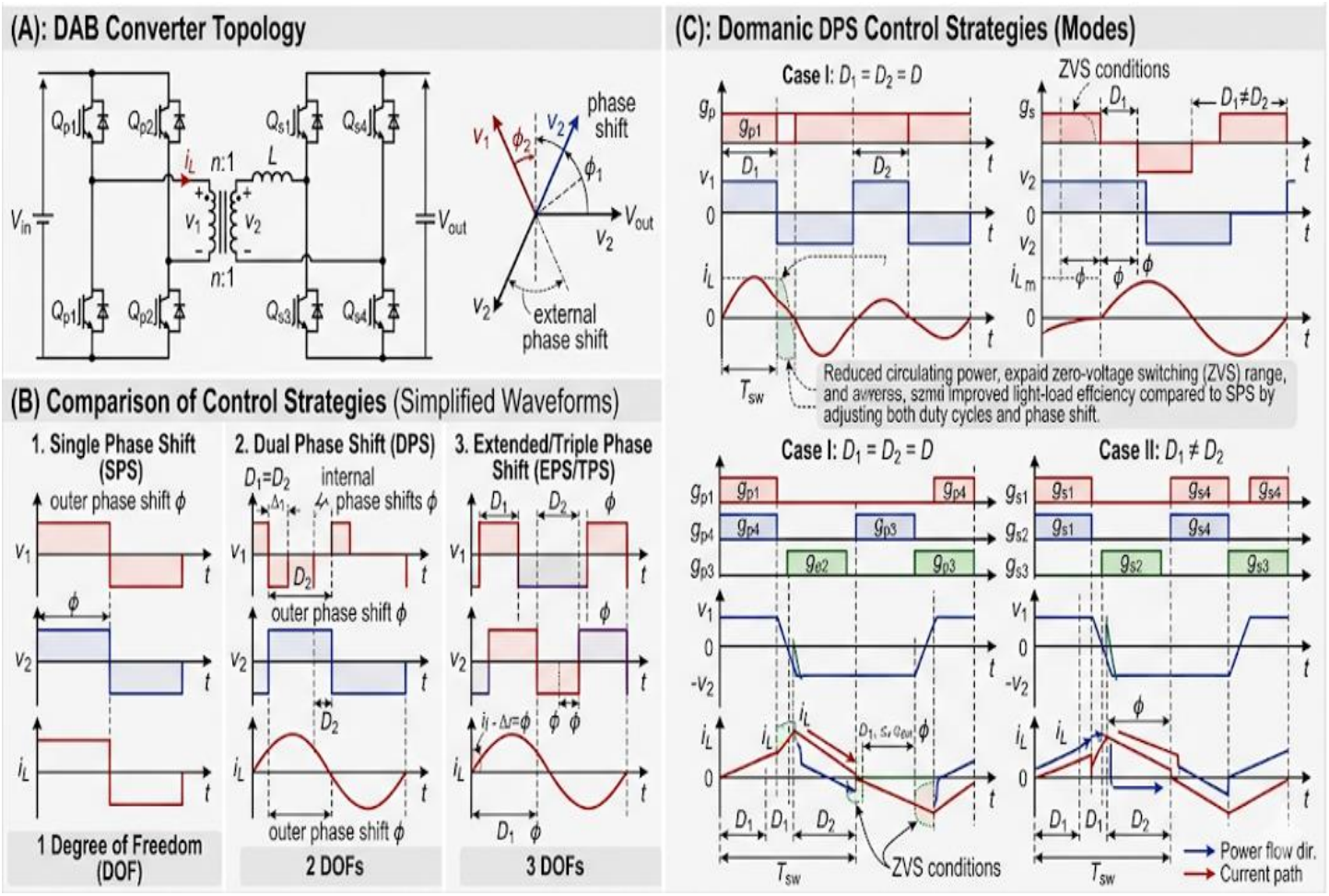

Figure 3: Operation diagrams of Dual Active Bridge using Triangular and Trapezium Modulation (TTM)(Shao, S.et al 2021 and Zhao, B et al 2013)

Figure 4 outlines the topology and operational waveforms of a bidirectional DAB converter, contrasting traditional Single-Phase Shift (SPS) modulation with multi-degree-of-freedom (DOF) strategies like Dual Phase Shift (DPS) and Extended/Triple Phase Shift (EPS/TPS). Although SPS depends exclusively on an outer phase-shift angle (ϕ), DPS and EPS introduce inner duty-cycle ratios (D_1 and D_2) to create zero-voltage intervals in the AC-link voltages ($v_1$and v_2). By controlling these additional DOFs, the converter changes the instantaneous volt-second balance across the leakage inductance L, driving the inductor current i_L into piecewise-linear trajectories that describe Triangular and Trapezium Modulation (TTM). As specified in Case I ($D_1 = D_2$) and Case II ($D_1 \neq D_2$) switching waveforms, shaping i_L into triangular or trapezoidal shapes during light-to-medium load conditions clearly curtails the backflow of reactive power and lowers circulating current. Critically, modifying the internal phase shifts guarantees that the switching changes match with good current polarities, thereby extensively increasing the ZVS boundaries across all active switches (Q_{P1}-Q_{P4} and Q_{s1}-Q_{s4}) and removing the light-load efficiency degradation of conventional SPS control.

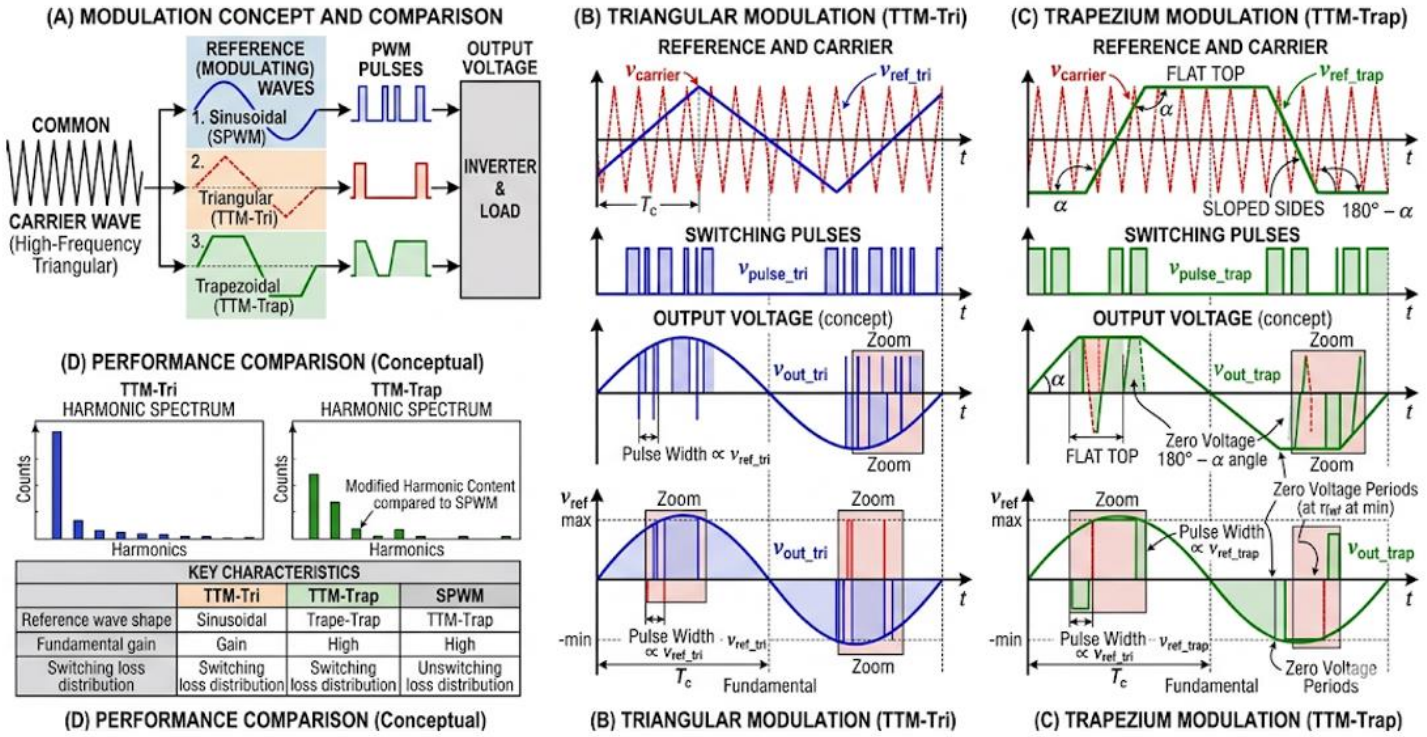

Figure 4: Diagrams of Triangular and Trapezium Modulation (TTM) Techniques (Holmes, D. G et al 2003, Wang, Y. C et al 2016)

Figure 5 illustrates the Triangular and Trapezoidal Modulation (TTM) scheme, combining TRM and TZM as discontinuous/boundary conduction strategies to optimize DAB converters during light loads or severe voltage mismatches. ($V_{in} \neq nV_{out}$). In Triangular Modulation, the two DAB bridge switching instances are specifically controlled such that the isolation inductor current. i_L commences at zero, rises linearly to a peak value throughout the active voltage pulse coordination of v_1 *and* v_2, and returns to zero before the half-switching cycle ends, staying inactive for the rest of the period. This zero-current boundary condition removes reactive back-flow power and ensures both ZVS and ZCS during turn-on and turn-off transitions, reducing high-frequency switching losses. Contrarywise, Trapezoidal Modulation extends the current conduction interval by incorporating a flat plateau where v_1 matches the reflected secondary voltage nv_1, essentially bounding the peak inductor current while maintaining the RMS current profile significantly lower than the traditional Single-Phase-Shift (SPS) modulation under identical conditions. By dynamically alternating between these triangular and trapezoidal current trajectories based on the instantaneous voltage gain and load demand, the converter decreases total conduction and switching losses, keeping peak efficiency across a very wide operational envelope.

e. PWM Plus Phase Shift (PWM–PS)/ Extended Phase Shift (EPS) technique

PWM–PS technique is a multi-degree-of-freedom modulation technique improved to resolve the fundamental efficiency weaknesses of traditional SPS modulation. In this architecture, both the duty cycle and phase shift are concurrently adjusted. One of the two bridges (primary or secondary) is modulated with an internal pulse-width ($D_p$or D_s), while the other remains at a fixed 50% duty cycle, with a global phase shift ϕ regulating the inter-bridge power flow. This creates a three-level voltage waveform on one side and a two-level square wave on the other, leading to a hybrid excitation of the linkage inductor L. The power transfer expression under PWM–PS is given by equation (8) [36]. By controlling these variable quantities along with the displacement angle ϕ, the controller can precisely shape the inductor current. $i_L(t)$ to meet the required power demand while reducing parasitic losses. PWM-PS offers reduced circulating current compared to PSM. In traditional SPS, each time $M \neq 1$, a section of the inductor current flows in opposition to the bridge voltage, creating backflow power that cycles through the components without reaching the load. PWM–PS employs the internal duty cycle to blank the voltage during high-reactive times [37]. This suppresses the reactive power component, leading to reduced RMS current values and consequently I^2R losses in the transformer and power (MOSFETs) semiconductors. PSM encounters a tight ZVS range, specifically at light loads. PWM–PS mitigates this constraint by introducing an extra control variable to guarantee the inductor current at the switching transitions fully discharges the switch output capacitances (C_{oss}) [8]. By changing the duty cycle, the converter keeps ZVS even when there is a substantial input and output voltage mismatch. This eliminates the switching loss effect (12) that forces a decrease in switching frequency.

$$P_{sw} = 0.5C_{oss}V^2f_{sw} \qquad (12)$$

PWM introduction into the bridge voltage changes the fundamental component of the excitation waveform, resulting in increased harmonic distortion [13]. The successive quasi-square wave has higher-order harmonics that increase AC winding losses due to skin and proximity effects in the transformer, thereby necessitating a more complicated magnetic design than the pure 50% duty-cycle

square waves applied in SPS/PWM. PWM–PS increases control complication relative to SPS, as the controller should compute the real-time optimal duty cycle (D) for all power levels and voltage ratio (M) [6]. This imposes precomputed look-up tables or complex piecewise control algorithms for smooth transitions across operating modes, such as shifting from PWM–PS under light-load conditions to SPS at full load [38].

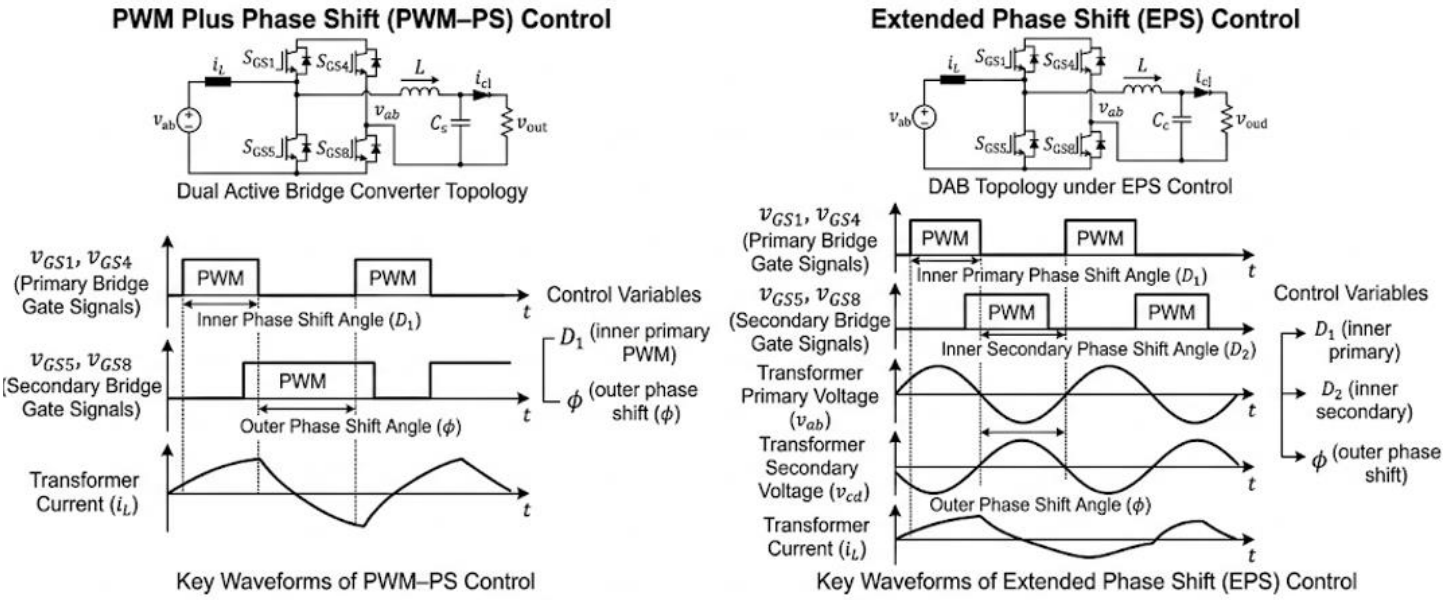

Table: Comparison of Control Techniques

Technique	Standard SPS	PWM–PS	D_1, D_2, ϕ	EPS
Degrees of Freedom	ϕ only	D_1, ϕ	Two	Three
Primary Benefit	Simplicity	One	Reduced Backflow Power	Enhanced Efficiency & Power Range

Figure 5: Comparison of PWM Plus Phase Shift (PWM-PS) and Extended Phase Shift (EPS) Control Techniques for Dual Active Bridge (Xu, D.et al 2004, Zhao, B. et al 2015)

Figure 6 demonstrates the Extended Phase Shift (EPS) Dual Active Bridge converter topology, which improves power distribution by adding an inner phase-shift variable (D_1,). Distinct from the standard SPS control, where the primary and secondary bridges produce fixed 50% duty cycles, EPS changes one bridge to synthesize a three-level AC output (v_1) that includes a zero-voltage state. The other bridge generates a two-level square wave (v_2), with power transfer governed by the outer phase shift (D_2 or ϕ). Controlling both degrees of freedom (D_1 and D_2) balances the inductor (L) volt-second product, shaping the piece-wise linear current (i_L) trajectory. This advanced modulation eliminates the reactive back-flow power and reduces peak and RMS conduction losses that otherwise degrade efficiency under severe voltage mismatch conditions ($V_{in} \neq nV_{out}$), thereby significantly increasing the soft-switching Zero Voltage Switching (ZVS) boundaries across the converter's full load profile.

f. Asymmetric Duty Cycle Control (ADC)

The Asymmetric Duty Cycle Control (ADC) technique for the DAB converter is a specialised modulation technique that optimizes efficiency when the DAB works under a wide range of voltage conversion ratios [39-40]. ADC encompasses the concurrent change of duty cycle and phase shift. In ADC, one or both bridges function with an asymmetric duty cycle (typically $D < 0.5$), altering the transformer excitation from a two-level square wave to a three-level quasi-square wave [9]. The power transfer is as given by (9). The phase shift ϕ remains the predominant variable for power flow direction and magnitude, yet D_p and D_s offer the required degrees of freedom to support the voltage pulses and current peaks. ADC decreases the circulating current compared to PSM. By employing asymmetric duty cycles, the zero-voltage states can be timed to match with these potential backflow cycles. This results in inductor current that is further in-phase with power transfer, resulting in minimal RMS current values and superior thermal performance of the MOSFETs and transformer. ADC is effective in maintaining ZVS over a wide operational range by dynamically varying duty cycles to guarantee adequate instantaneous current during switching changes to fully discharge and charge the output capacitances of the power devices [41]. This offers improved performance in comparison to SPS, which often fails ZVS in light-load conditions or substantial voltage mismatch, leading to hard-switching losses. However, its asymmetric modulation introduces DC flux bias in the transformer if unbalanced, unlike the intrinsically symmetric 50% duty-cycle PSM operation. This demands high-precision gate timing and active flux balancing algorithms to avoid core saturation. Even inferior timing mismatches between positive and negative pulses gather a DC component in the inductor current [42]. Furthermore, since both duty cycle and phase shift are simultaneously controlled, ADC requires a modern control framework that solve real time multi-variable optimization problems, increasing computational complexity compared to the single-variable PSM phase-shift control [43]. Moreover, the quasi-square waveform

formed by ADC has a higher harmonic spectrum compared to an ordinary square wave, while useful for current shaping and RMS reduction, these higher harmonics increase AC winding losses due to skin and proximity effects [9, 44].

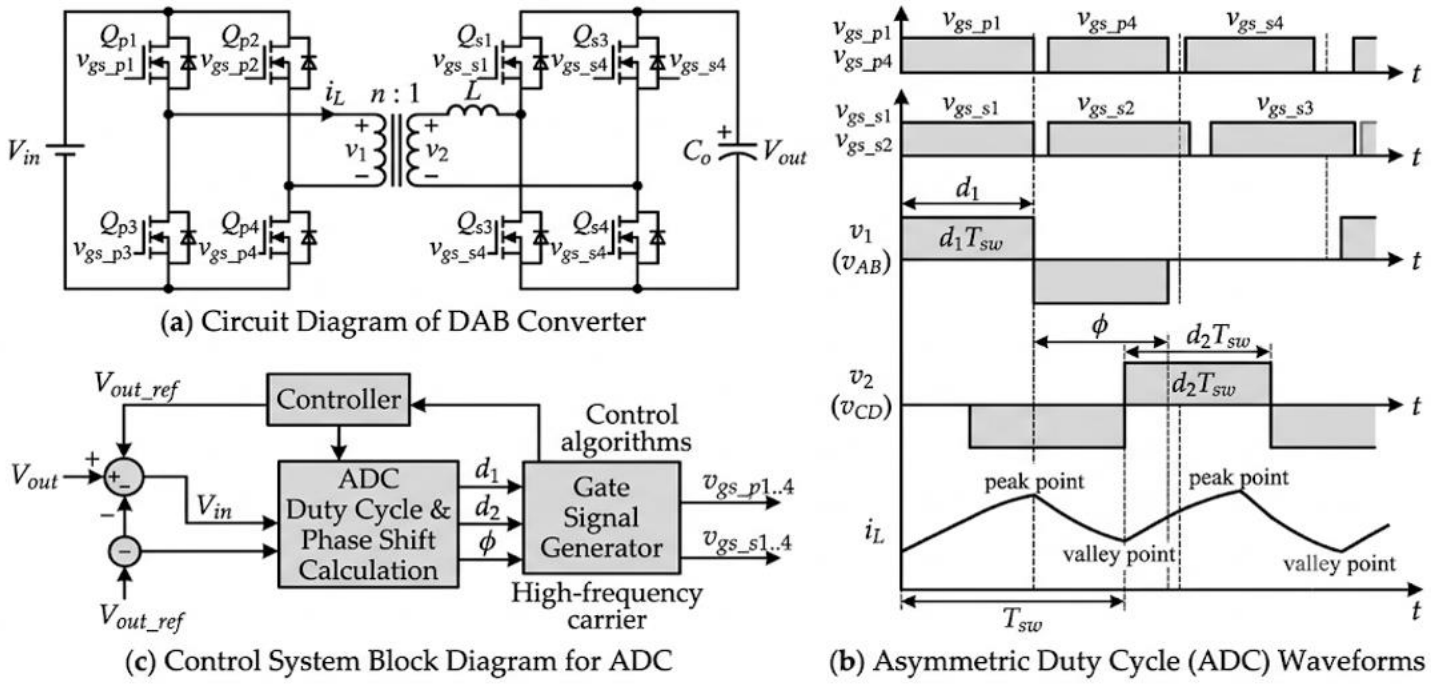

Figure 6: Asymmetric Duty Cycle Control (ADC) for Dual Active Bridge Converter (Liu, P. et al 2025, Wang, L. et al 2011)

Figure 7 describes a DAB converter Asymmetric Duty Cycle Control (ADC) framework, showing how introducing additional degrees of freedom improves bidirectional power conversion. As shown in the circuit diagram (a), the system comprises a primary and secondary active full-bridge isolated by an n: 1 high-frequency transformer, where the instantaneous energy transfer is governed by the voltage differential across the auxiliary inductor L. Unlike traditional single-phase-shift modulation, the ADC waveforms in (b) utilize three independent variables the primary duty cycle d_1, the secondary duty cycle d_2, and the phase shift ϕ to eliminate the volt-second mismatch across the inductor that typically occurs under wide voltage variations. This precise asymmetric modulation shapes the piece-wise linear trajectory of the inductor current $i_L$between its peak and valley points, which drastically minimizes reactive circulating power and ensures Zero Voltage Switching (ZVS) across a significantly broader operating envelope. To execute this multi-variable optimization, the control architecture in (c) processes the output voltage error and input/output feedforward variables through an ADC calculation block, which dynamically solves for the optimal (d_1, d_2, ϕ) triplet to maximize efficiency before a gate signal generator synthesizes the precise asymmetric high-frequency PWM driving signals ($v_{gs\_p1\ldots4}, v_{gs\_s1\ldots4}$).

III. CRITICAL ANALYSIS AND SUMMARY OF FINDINGS

The technical evaluation of DAB converter PWM techniques shows a clear trade-off between control simplicity and operational efficiency. Conventional PSM operates as a standard, presenting great simplicity by using a single degree of freedom and the phase displacement angle ϕ. However, PSM presents significant performance degradation in voltage mismatch conditions ($M \neq 1$), which is typical in electric vehicle (EV) lithium-ion battery cycles. This gap triggers a surge in circulating power and a collapse of the ZVS range [45]. Technically, as M diverges from unity, the reactive power component rises, leading to backflow power where energy returns to the source within each half-cycle, scaling conduction losses by I_{rms}^2. Advanced methods such as CPWM and ADC resolve these flaws by ensuring that bridge voltages are not fixed at 50% duty. By simultaneously changing the duty cycle and phase shift, these techniques generate three-level quasi-square waves that decouple voltage magnitude from the switching period. This multi-dimensional control space permits the reduction of circulating current by zeroing out bridge voltages throughout potential backflow periods. Specifically, the power transfer follows a more complex interaction, as defined in (8) and (9). For functions requiring high efficiency over wide voltage trajectories, such as fast DC charging, DPS and PWM–PS present excellent performance [46]. DPS introduces an equal inner phase shift to the two bridges, which substantially suppresses circulating current and facilitates a wide ZVS range. PWM–PS further enhances this by modulating only one bridge's duty cycle, providing a very wide ZVS range and very low circulating current, making it standard for ultra-fast DC charging infrastructure. Equally, TTM offers a dedicated solution for light-to-medium power levels. By limiting the current waveform to specific shapes, TTM removes turn-off losses via Zero-Current Switching (ZCS). While TTM is arguably the most efficient method to handle backflow power, it imposes remarkably higher peak current stress on semiconductor MOSFET devices and transformer cores [47]. The comparative performance analysis of the various modulation

techniques in relation to EV Charging is outlined in Table 1. The table shows a clear correlation between control complexity and operational efficiency in EV charging applications. While PSM establishes low control complexity and moderate efficiency appropriate for medium-power On-Board Chargers (OBC), it incurs high circulating currents at light loads. Distinct from the contemporary PWM strategies such as DPS, PWM–PS attain high to very high efficiency and very low circulating currents by leveraging wide Zero Voltage Switching (ZVS) ranges, giving these techniques highly practical for high-performance infrastructure [48]. Strategies such as CPWM and ADC offer a reasonable trade-off, offering medium control complexity with high efficiency for bidirectional and slow DC charging systems. Ultimately, TTM and PWM–PS stand out for high-power demands due to exceptional ZVS performance and reduced power losses, albeit at the cost of considerably higher implementation complexity.

TABLE 1: COMPARATIVE PERFORMANCE ANALYSIS OF THE VARIOUS MODULATION TECHNIQUES IN RELATION TO EV CHARGING

Technique	ZVS Range	Circulating Current	Efficiency	Control Complexity	Suitability for EV Charging
PSM	Medium	High at light load	Moderate	Low	Medium-power OBC
CPWM	Medium–Wide	Medium	High	Medium	OBC and slow DC
DPS	Wide	Low	Very High	High	Fast DC chargers
TTM	Wide	Low	High	High	High-power DC
PWM–PS	Very Wide	Very Low	Very High	High	Ultra-fast DC
ADC	Medium–Wide	Medium	High	Medium	Bidirectional chargers

TABLE 2: ANALYSIS OF THE VARIOUS MODULATION TECHNIQUES USED TO MANAGE POWER FLOW AND EFFICIENCY IN DUAL ACTIVE BRIDGE (DAB) CONVERTERS.

Technique	*Control Variables*	*Voltage Waveform Type*	*Primary Benefit*	*Technical Drawback*
Phase Shift Modulation (PSM/SPS)	*Single (ϕ)*	*2-Level Square*	*Extreme simplicity in control and implementation.*	*High circulating current and narrow ZVS range when $V_1 \neq nV_2$*
Combined PWM (CPWM)	*Multiple (ϕ, D_p, D_s)*	*3-Level Quasi-Square*	*Reduced circulating current compared to PSM*	*High computational overhead: duty cycles and phase shift are simultaneously varied*
Dual Phase Shift (DPS)	*Dual (ϕ, D_1)*	*3-Level Quasi-Square*	*Significant reduction in backflow power; expanded ZVS envelope.*	*Requires precise timing to avoid DC offset; complex mathematical mapping*
Triangular/ Trapezium (TTM)	*Multiple (ϕ, D_p, D_s)*	*Triangular / Trapezoidal*	*Eliminates switching losses via ZCS; ideal for light loads.*	*Very high peak current stress; limited to low-to-medium power levels.*
PWM plus Phase Shift (PWM–PS)	*Multiple (ϕ, D_p, D_s)*	*Hybrid (2-Level & 3-Level)*	*Optimized efficiency by adjusting one bridge's duty cycle.*	*Power Transfer follows $P = \frac{V_1 V_2}{\omega L}(D_P D_S) f(\phi)$: complex mode transitions*
Asymmetric Duty Cycle (ADC)	*Multiple (ϕ, D_p, D_s)*	*3-Level Quasi-Square*	*Efficiently handles wide voltage gain variations in EV systems.*	*Bridges are no longer fixed at 50% duty; risk of transformer flux imbalance.*

Table 2 examines the various DAB modulation strategies, showing the key trade-off between control complexity and operational efficiency. While PSM offers intense implementation simplicity, its high circulating currents and narrow ZVS range at mismatched voltage levels ($V_1 \neq nV_2$) require the use of complex multi-variable strategies. Strategies like DPS and CPWM employ 3-level quasi-square waveforms to drastically reduce backflow power and increase the ZVS envelope, albeit at the cost of higher computational overhead and complex mathematical mapping. Also, specific methods like TTM eliminate switching losses via ZCS for light-load optimization, while ADC and PWM–PS offer enhanced efficiency for wide voltage gain variations typical in EV systems [49]. Despite these operational benefits, these modern modulation techniques introduce technical challenges, for instance, high peak current stress, complex mode transitions, and potential transformer flux imbalance. The images in Figure 8 demonstrate the advancement of phase-shift modulation strategies for a DAB converter from SPS to EPS, DPS, and ultimately Triple Phase Shift (TPS) modulation by consecutively increasing the control degrees of freedom from one to three. While the baseline SPS modulation depends exclusively on a single outer phase shift between two-level square waves, the advanced schemes present independent inner phase shifts to generate three-level AC voltage waveforms (v_{h1} and v_{h2}) on the bridges. This additional control flexibility changes the slope and trajectory of the high-frequency inductor current (i_L), systematically decreasing the circulating current zones (highlighted in yellow) and curtailing reactive power. Eventually, migrating from SPS toward the fully decoupled TPS architecture offers the mathematical degrees of freedom essential to optimize the converter's efficiency profile, significantly reducing RMS conduction losses and expanding the ZVS range under mismatched voltage ratios. Beyond the optimization of macro-level modulation parameters, the operational efficacy of advanced multi-degree-of-freedom (multi-DOF) Pulse Width Modulation (PWM) strategies is fundamentally coupled with the transient dynamics of the dead-time interval. Traditional fixed dead-time allocation introduces a severe performance trade-off across the wide voltage and load variations characteristic of electric vehicle (EV) charging cycles. Under light-load conditions, an uncompensated, fixed dead-time interval is frequently insufficient for the reduced instantaneous inductor current $i_L(t)$ to completely charge or discharge the MOSFET switch output capacitances C_{oss}, resulting in a loss of Zero-Voltage Switching (ZVS) and inducing hard-switching losses. Conversely, excessively long fixed intervals during high-power operation provoke prolonged body-diode conduction, escalating reverse-recovery losses and causing significant phase-shift distortion that destabilizes the pre-calculated, optimized multi-variable trajectories (d_1, d_2, ϕ). To alleviate these non-idealities and remove the bridge shoot-through risk, the integration of current-aware adaptive dead-time control becomes imperative. By dynamically calculating the precise commutation

interval as a function of the peak or valley switching currents, C_{oss} non-linearities, and fluctuating DC-link boundaries, the adaptive dead-time mechanism ensures complete soft-switching commutation across the entire battery operating envelope while preserving the exact mathematical integrity of the underlying advanced PWM control law.

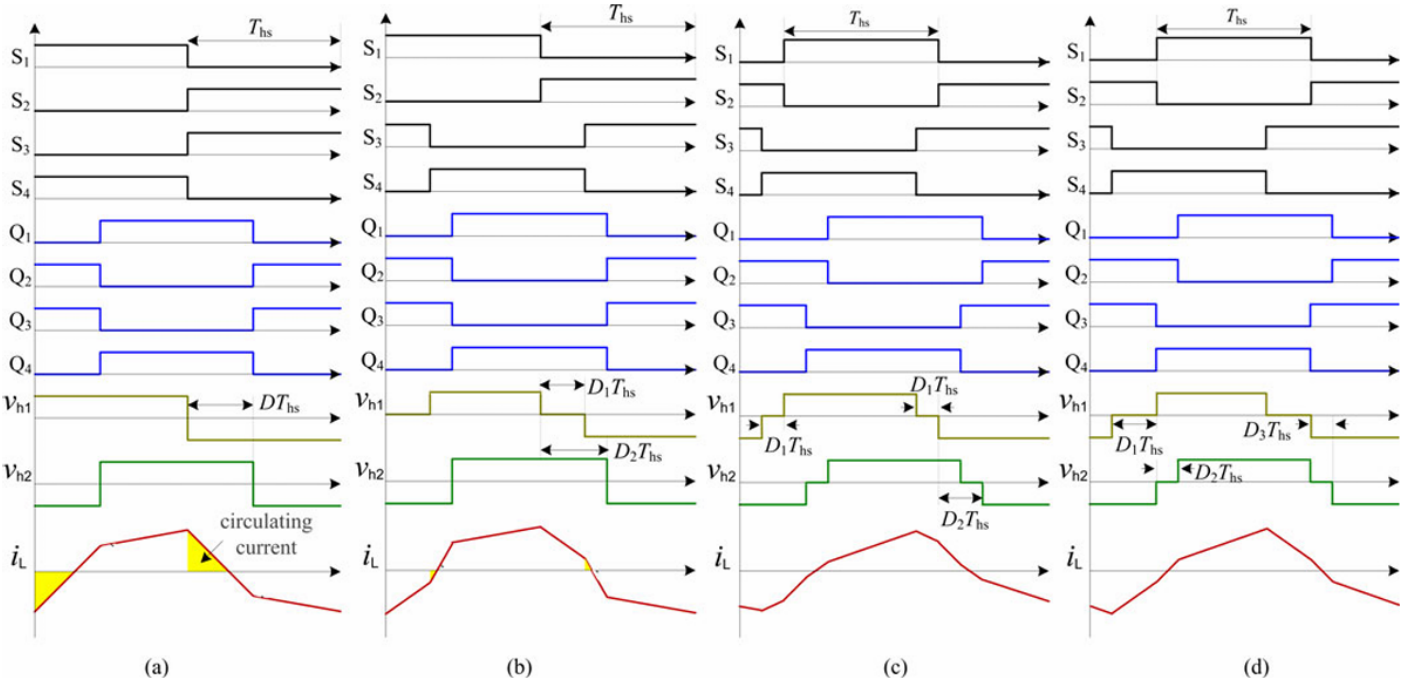

Figure 7: Progression of DAB converter phase-shift modulation strategies (SPS, EPS, DPS, TPS) with increasing degrees of freedom (Shao, S. et al 2021, Zhao, B. et al 2014)

IV. CONCLUSION

The paper has concluded that a sufficiently selected modulation technique is essential in enhancing the DAB efficacy implemented in EV charging systems. Even though PSM continues to be technically attractive in medium-power chargers due to its low control complexity, its application has decreased in high-performance units due to sensitivity issues to high circulating inductive currents and hard-switching during voltage gaps. Modern modulation strategies, *inter alia*, CPWM, DPS, TTM, PWM–PS, and ADC, pose the crucial degrees of freedom to improve the current trajectory and boost the soft-switching envelope. DPS and PWM–PS appear as the strongest contenders for fast and ultra-fast DC charging, depicting high efficiency (>95%) and advanced functioning across wide battery voltage ranges. However, these benefits come at the cost of increased computational complexity and potential dangers such as DC flux bias in the transformer. Eventually, the selection of a PWM technique must balance the definite conditions of power density, efficiency, and hardware cost to satisfy the strict demands of V2G EV infrastructure.

REFERENCES

1. A. V. Mirtchev and E. C. Tatakis, "Design methodology based on dual control of a resonant dual active bridge converter for electric vehicle battery charging," *IEEE Trans. Veh. Technol.*, vol. 71, no. 3, pp. 2691–2705, Mar. 2022.
2. F. Jarraya, A. Khan, A. Gastli, L. Ben-Brahim, and R. Hamila, "Design considerations, modelling, and control of dual-active full bridge for electric vehicles charging applications," *The J. Eng.*, vol. 2019, no. 12, pp. 8439–8447, Dec. 2019.
3. S. H. Kuo *et al.*, "High efficiency dual-active-bridge converter with triple-phase-shift control for battery chargers of electric vehicles," *Energies*, vol. 17, no. 2, p. 354, Jan. 2024.
4. K. Kuroda, M. Ogura, H. Maeji, M. Oe, G. Toyoda, and N. Kurio, "DC Distribution System for Improved Power System Resilience with Renewable Energy," *SEI Tech. Rev.*, no. 91, p. 59, 2020.
5. X. Liu *et al.*, "Novel dual-phase-shift control with bidirectional inner phase shifts for a dual-active-bridge converter having low surge current and stable power control," *IEEE Trans. Power Electron.*, vol. 32, no. 5, pp. 4095–4106, May 2016.
6. Z. Qin, Y. Shen, P. C. Loh, H. Wang, and F. Blaabjerg, "A dual active bridge converter with an extended high-efficiency range by DC blocking capacitor voltage control," *IEEE Trans. Power Electron.*, vol. 33, no. 7, pp. 5949–5966, Jul. 2017.

7. M. N. Kheraluwala, R. W. Gascoigne, D. M. Divan, and E. D. Baumann, "Performance characterization of a high-power dual active bridge DC-to-DC converter," *IEEE Trans. Ind. Appl.*, vol. 28, no. 6, pp. 1294–1301, Nov./Dec. 1992.
8. S. Shao *et al.*, "Modeling and advanced control of dual-active-bridge DC–DC converters: A review," *IEEE Trans. Power Electron.*, vol. 37, no. 2, pp. 1524–1547, Feb. 2021.
9. D. Lyu, C. Straathof, T. B. Soeiro, Z. Qin, and P. Bauer, "ZVS-optimized constant and variable switching frequency modulation schemes for dual active bridge converters," *IEEE Open J. Power Electron.*, vol. 4, pp. 801–816, 2023.
10. P. Liu, S. Yu, R. Zhang, Y. Cheng, and S. Yu, "Analysis and Compensation of Dead-Time Effect in Dual Active Bridge with Asymmetric Duty Cycle," *Symmetry*, vol. 17, no. 10, p. 1701, 2025.
11. V. N. Saraswathi and V. P. Ramachandran, "A comprehensive review on charger technologies, types, and charging stations models for electric vehicles," *Heliyon*, vol. 10, no. 20, 2024.
12. F. Krismer, S. Round, and J. W. Kolar, "Performance optimization of a high current dual active bridge with a wide operating voltage range," in Proc. 37th IEEE Power Electronics Specialists Conf. (PESC), Jun. 2006, pp. 1–7.
13. D. Xu, C. Zhao, and H. Fan, "A PWM plus phase-shift control bidirectional DC-DC converter," *IEEE Trans. Power Electron.*, vol. 19, no. 3, pp. 666–675, May 2004.
14. B. Zhao, Q. Yu, and W. Sun, "Extended-phase-shift control of isolated bidirectional DC–DC converter for power distribution in microgrid," *IEEE Trans. Power Electron.*, vol. 27, no. 11, pp. 4667–4680, Nov. 2011.
15. B. Zhao, Q. Song, and W. Liu, "Power characterization of isolated bidirectional dual-active-bridge DC–DC converter with dual-phase-shift control," *IEEE Trans. Power Electron.*, vol. 27, no. 9, pp. 4172–4176, Sep. 2012.
16. A. K. Jain and R. Ayyanar, "PWM control of dual active bridge converters," U.S. Patent 8,587,975, Nov. 19, 2013.
17. V. Timmers, A. Egea-Àlvarez, A. Gkountaras, and L. Xu, "Multi-objective optimization and comparison of DC/DC converters for offshore wind turbines," *IEEE Access*, vol. 12, pp. 81236–81251, 2024.
18. B. Zhao, Q. Song, W. Liu, and Y. Sun, "Overview of dual-active-bridge isolated bidirectional DC–DC converter for high-frequency-link power-conversion system," *IEEE Trans. Power Electron.*, vol. 29, no. 8, pp. 4091–4106, Aug. 2013.
19. S. Darnal, "A study on single phase-shift high-power dual active bridge (dab) converter for PV application," Research Report, 2024.
20. F. Xie, H. Wang, and J. Shu, "Backflow power optimization of DAB based on asymmetric duty cycle and internal phase shift control," *IEEE Access*, vol. 11, pp. 25682–25688, 2023.
21. B. Zhao, Q. Yu, and W. Sun, "Extended-phase-shift control of isolated bidirectional DC–DC converter for power distribution in microgrid," *IEEE Trans. Power Electron.*, vol. 27, no. 11, pp. 4667–4680, Nov. 2011. *[Note: Duplicate entry of reference 14]*
22. S. Gao, Y. Zhang, Y. Wang, J. Liu, and D. Xu, "An optimal control strategy for the DAB-based partial power converter based on extended-phase-shift control," *IEEE Open J. Power Electron.*, vol. 4, pp. 817–827, 2023.
23. S. Shi *et al.*, "Research on optimum extended phase-shift control with minimum peak-to-peak current of DAB converter applied to small DC power grid," *Front. Energy Res.*, vol. 10, p. 1115146, 2023.
24. K. Shen *et al.*, "ZVS Control strategy of dual active bridge DC/DC converter with triple-phase-shift modulation considering RMS current optimization," *The J. Eng.*, vol. 2019, no. 18, pp. 4708–4712, 2019.
25. H. Wen, W. Xiao, and B. Su, "Nonactive power loss minimization in a bidirectional isolated DC–DC converter for distributed power systems," *IEEE Trans. Ind. Electron.*, vol. 61, no. 12, pp. 6822–6831, Dec. 2014.
26. J. Hu, Z. Yang, S. Cui, and R. W. De Doncker, "Closed-form asymmetrical duty-cycle control to extend the soft-switching range of three-phase dual-active-bridge converters," *IEEE Trans. Power Electron.*, vol. 36, no. 8, pp. 9609–9622, Aug. 2021.
27. C. Song, A. Chen, Y. Pan, C. Du, and C. Zhang, "Modeling and optimization of dual active bridge dc-dc converter with dead-time effect under triple-phase-shift control," *Energies*, vol. 12, no. 6, p. 973, 2019.
28. H. Yunfei, Z. Qihao, and O. Youpeng, "Overview of topologies and control strategies for dual-active-bridge converters," *J. Power Supply*, vol. 22, no. 4, pp. 53–65, 2024.
29. H. van Hoek, M. Neubert, and R. W. De Doncker, "Enhanced modulation strategy for a three-phase dual active bridge—Boosting efficiency of an electric vehicle converter," *IEEE Trans. Power Electron.*, vol. 28, no. 12, pp. 5499–5507, Dec. 2013.
30. G. Oggier, G. O. Garcia, and A. R. Oliva, "Modulation strategy to operate the dual active bridge DC-DC converter under soft switching in the whole operating range," *IEEE Trans. Power Electron.*, vol. 26, no. 4, pp. 1228–1236, Apr. 2010.
31. Y. C. Wang, F. M. Ni, and T. L. Lee, "Hybrid modulation of bidirectional three-phase dual-active-bridge DC converters for electric vehicles," *Energies*, vol. 9, no. 7, p. 492, 2016.
32. A. K. Bhattacharjee and I. Batarseh, "Optimum hybrid modulation for improvement of efficiency over wide operating range for triple-phase-shift dual-active-bridge converter," *IEEE Trans. Power Electron.*, vol. 35, no. 5, pp. 4804–4818, May 2019.
33. P. B. Musiiwa, E. T. Kapuya, D. Musdemba, and S. Akashe, "Analysis and Mitigation of Shoot-Through in Dual Active Bridge MOSFET Converters for EV Chargers," in Proc. IEEE 5th Int. Conf. ICT in Business Industry & Government (ICTBIG), Dec. 2025, pp. 1–5.
34. D. D. Nguyen, T. T. Pham, T. T. Le, S. Choi, and K. Yukita, "A modulation method for three-phase dual-active-bridge converters in battery charging applications," *Sustainability*, vol. 15, no. 6, p. 5170, 2023.

35. M. H. A. bin Ab Malek, H. Kakigano, and K. Takaba, "Combined Pulse-Width Modulation of Dual Active Bridge DC-DC Converter to Increase the Efficiency of Bidirectional Power Transfer," *IEEJ J. Ind. Appl.*, vol. 7, no. 2, pp. 166–174, 2018.
36. H. A. B. A. M. Muhammad and K. Hiroaki, "Combined pulse-width Modulation of dual active bridge DC-DC converter to reduce circulating current at bidirectional power transfer," *IEEJ J. Ind. Appl.*, 2017.
37. M. H. A. bin Ab Malek, H. Kakigano, and K. Takaba, "Dual Active Bridge DC-DC Converter with Tunable Dual Pulse-Width Modulation for Complete Zero Voltage Switching Operation," *IEEJ J. Ind. Appl.*, vol. 8, no. 1, pp. 98–107, 2019.
38. H. Bai, C. C. Mi, S. Wang, and S. Garg, "The modeling and control of a ZVS bidirectional DC-DC converter with phase-shift plus PWM control scheme," *IEEE Trans. Power Electron.*, vol. 23, no. 2, pp. 813–823, Mar. 2008.
39. F. Jauch and J. Biela, "Combined phase-shift and frequency modulation of a dual-active-bridge AC–DC converter with PFC," *IEEE Trans. Power Electron.*, vol. 31, no. 12, pp. 8387–8397, Dec. 2016.
40. B. Zhao, Q. Song, W. Liu, G. Liu, and Y. Zhao, "Universal high-frequency-link characterization and practical fundamental-optimal strategy for dual-active-bridge DC-DC converter under PWM plus phase-shift control," *IEEE Trans. Power Electron.*, vol. 30, no. 12, pp. 6488–6494, Dec. 2015.
41. C. Gu, Z. Zheng, Y. Li, X. Liu, and P. Wheeler, "General modulation optimization methods of dual-active-bridge (DAB) converters," in Proc. IECON 2017 - 43rd Annu. Conf. IEEE Ind. Electron. Soc., Oct. 2017, pp. 4920–4925.
42. L. Wang, Z. Wang, and H. Li, "Asymmetrical duty cycle control and decoupled power flow design of a three-port bidirectional DC-DC converter for fuel cell vehicle application," *IEEE Trans. Power Electron.*, vol. 27, no. 2, pp. 891–904, Feb. 2011.
43. S. Nakahara *et al.*, "Development of dual active bridge dc-dc converter to achieve high efficiency in wide voltage and load range and application to v2h systems," *IEEJ J. Ind. Appl.*, vol. 13, no. 4, pp. 475–488, 2024.
44. R. Yamada, A. Hino, and K. Wada, "Improvement of efficiency in bidirectional DC-DC converter with dual active bridge using GaN-HEMT," *IEEJ J. Ind. Appl.*, vol. 12, no. 3, pp. 264–272, 2023.
45. C. Cui, D. Pehrman, Y. Liu, and Q. Zhang, "Zero voltage switching for high power three-phase inductive power transfer with a dual active bridge," *IEEE Access*, vol. 12, pp. 7121–7133, 2024.
46. M. M. Rana *et al.*, "Comprehensive review on the charging technologies of electric vehicles (EV) and their impact on power grid," *IEEE Access*, vol. 13, pp. 35124–35156, 2025.
47. G. Chen, Z. Chen, Y. Chen, F. C. Feng, and X. Zhu, "Asymmetric phase-shift modulation strategy of DAB converters for improved light-load efficiency," *IEEE Trans. Power Electron.*, vol. 37, no. 8, pp. 9104–9113, Aug. 2022.
48. F. An, W. S. Song, and K. X. Yang, "Optimised power control with extended phase shift in dual-active-bridge dc–dc converters," *Electron. Lett.*, vol. 54, no. 10, pp. 651–653, 2018.
49. S. S. Shah, V. M. Iyer, and S. Bhattacharya, "An approach to unified full-order modeling of dual active bridge type converters," in Proc. IECON 2018 - 44th Annu. Conf. IEEE Ind. Electron. Soc., Oct. 2018, pp. 986–992.